Electrochimica Acta, Vol.25, p. 479.
Pergamon Press Ltd. 1980. Printed in Great Britain.

ERRATUM

P. Vitorge et M. Lamache, Obtention de sulfures de cuivre non stoechiométrique par voie électrolytique, analyse des solides par diffraction de rayons X, *Electrochimica Acta* **24**, 811 (1979).

In this paper, the equation on page 813, line 5 should read:

$$\delta_i = (Q_i/96{,}500)\,(1/2)\,(M/m).$$

Electrochimica Acta, Vol. 25, pp. 481–486.
Pergamon Press Ltd. 1980. Printed in Great Britain.

THE BEHAVIOUR OF A FIXED BED POROUS FLOW-THROUGH ELECTRODE DURING THE PRODUCTION OF *p*-AMINOPHENOL

F. GOODRIDGE and M. A. HAMILTON*
Department of Chemical Engineering, University of Newcastle upon Tyne,
Merz Court, Claremont Road, Newcastle upon Tyne, NE1 7RU, U.K.

(*Received* 28 *August* 1979)

Abstract – The behaviour of a fixed bed porous flow-through monel electrode has been investigated for the reduction of nitrobenzene to *p*-aminophenol in an aqueous acidic electrolyte and under essentially activation controlled conditions. Chemical yields have been determined experimentally as well as calculated from polarisation curves for a plane electrode. Potential and current distributions have been interpreted by means of a simple one-dimensional model.

NOMENCLATURE

a	Specific area of particulate electrode	cm^{-1}
a_o	Specific geometric area of particulate electrode	cm^{-1}
e	Effectiveness factor $= a/a_o$	dimensionless
F	Faraday constant	coulombs $gmol^{-1}$
i	Current density $= i_m + i_s$	$A\,cm^{-2}$
i_m	Current density of particulate phase	$A\,cm^{-2}$
i_o	Exchange current density (see text)	$A\,cm^{-2}$
i_s	Current density of electrolyte phase	$A\,cm^{-2}$
i_y	Current density at position y	$A\,cm^{-2}$
j	Reduced current density $= i_m/i$	dimensionless
K_m	Conductivity of particulate phase	$(\Omega\,cm)^{-1}$
K_s	Conductivity of electrolyte phase	$(\Omega\,cm)^{-}$
L	Width of electrode in the direction of current flow	cm
n	Number of electrons involved in reaction	dimensionless
R	Gas constant	$cal\,gmol^{-1}\,K^{-1}$
T	Temperature	C or K
x	Distance in the direction of current flow	cm
y	Reduced distance in the direction of current flow $= x/L$	dimensionless
α	Charge transfer coefficient	dimensionless
β	nF/RT	V^{-1}
δ	Defined by equation (4)	dimensionless
ε	Defined by equation (5)	dimensionless
ν	Defined by equation (12)	dimensionless
θ	Integration constant defined by equation (2)	dimensionless
ϕ	Electrode potential	V
ϕ'	$= \beta\phi$	dimensionless
ϕ_m	Potential of particulate phase	V
ϕ_s	Potential of electrolyte phase	V
ψ	Integration constant defined by equation (3)	dimensionless

INTRODUCTION

In recent years there has been great interest in so called fixed bed or porous flow-through electrodes (PFTE) where the working electrode consists of individual, electronically conducting, particles. Current flows to or from the bed by means of electronically conducting sheets, rods or gauze termed current feeders, the electrolyte passing through the porous spaces in the bed. Two important regimes can be distinguished depending on whether current and electrolyte flow are in parallel or at right angles to each other. The latter is often called a flow-by arrangement.

Most of the work on PFTE has been concerned with metal recovery and battery systems. Only a few authors[1–3] have investigated in depth the performance of a fixed bed for an organic reaction. In the present work the reduction of nitrobenzene in an acidic medium is used as a test reaction although the major product, *p*-aminophenol (*p*Ap), is of commercial interest. In consequence no attempt has been made to optimise its chemical yield by working at a high temperature and making accurate experimentation more uncertain. The reaction itself was chosen because products are highly potential dependent and the basic aim of the work was to relate the product yield observed on a plane electrode to that obtained with the PFTE, by taking into account the electrode potential distribution in the three-dimensional electrode. Additionally, it was hoped to predict electrode potential and current distribution in the PFTE by means of a mathematical model.

THE REACTION

The electrochemical reduction of nitrobenzene in acidic media has been the subject matter of many papers and a more detailed literature survey can be found in reference[4]. A systematic investigation by Wilson and Udupa[5] produced chemical yields of *p*Ap of 50–60%, using amalgamated copper or monel electrodes, 30% aqueous sulphuric acid and a temperature range of 80–90°C. Their results are substantially confirmed by other workers[6–8] employing non-

* Now with DuPont Research Centre, Kingston, Ontario, Canada.

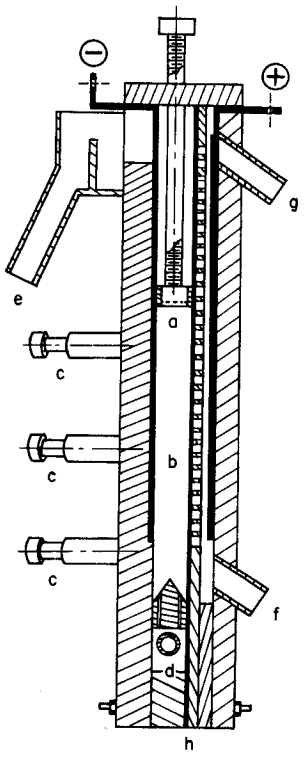

Fig. 1. Drawing of fixed bed cell. a: bed retainer; b: bed chamber; c: potential probe fixtures; d: catholyte inlet; e: catholyte outlet; f: anolyte inlet; g: anolyte outlet and h: ion exchange membrane.

amalgamated copper and monel electrodes. For an acidic medium potentiostatic investigations by Fleischmann *et al*[9] proposed the following overall reaction scheme which was based on their own and other workers' experiments:

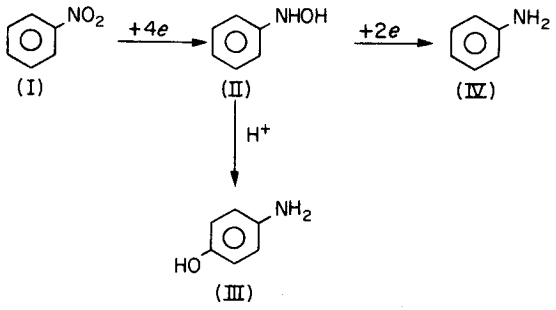

At low cathodic electrode potentials, nitrobenzene(I) is reduced directly to *N*-phenylhydroxylamine(II) which rearranges in acid to form *p*-aminophenol(III). At higher cathodic potentials the further reduction of (II) to aniline(IV) competes with the chemical rearrangement, which is favoured by high temperatures[10].

EXPERIMENTAL

Again fuller detail can be found in ref.[4].

Cells and equipment

Some preliminary results were obtained with a standard glass "H" cell, but most of the work used the cell shown in Fig. 1, made essentially from polypropylene with TPX (polymethylpentene) windows. Since catholyte flow was in an upwards direction, provision was made for restraining the cathode particles to prevent expansion of the bed. It should be noted that the geometry of the cell is such that electrolyte flows at right angles to the current, *ie* a flow-by arrangement. Figure 1 is drawn approximately to scale, the height of the packed section being 30 cm and its thickness 2.5 cm. Anolyte and catholyte compartments were separated by a cationic ion-exchange membrane (Ionac MC-3470), the anolyte being 25% sulphuric acid, the catholyte containing molar sulphuric acid. Cathode current feeder and bed particles were made of monel 400 alloy, the dimensionally stable anode[11] being in the form of a grid. Potential probes were introduced from the side (Fig. 1), Luggins being made of glass whilst probes for measuring metal potentials consisted of insulated steel tubing (1 mm i.d.) with a bare monel tip.

Figure 2 presents a schematic flow diagram of the rig which as indicated incorporated symmetrical anolyte and catholyte flow circuits.

Instrumentation

Most experiments used a Chemical Electronics type 50/20A potentiostat in an amperostatic mode. Potentials were determined by means of a Solartron A 211 digital voltmeter in conjunction with a Solartron–Schlumberger data transfer and analogue scanner, type 3215. All electrolyte potentials quoted in the present paper have been measured and are expressed with respect to a saturated calomel reference electrode.

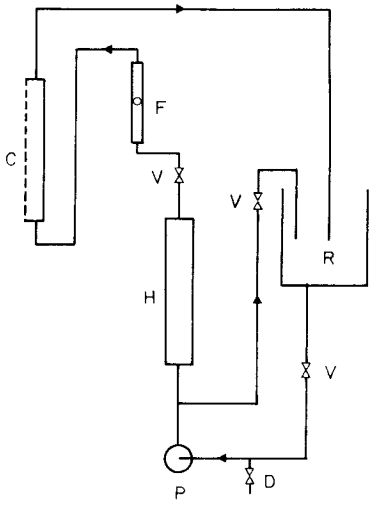

Fig. 2. Schematic drawing of catholyte and anolyte flow circuit. C: cell section; D: drain valve; H: heat exchanger; P: pump; F: flow meter; R: reservoir and V: flow control valve.

Materials

All reagents were B.D.H. Analar grade. Singly distilled water was used throughout the work.

Procedure

In all runs the nitrobenzene concentration was kept as constant as possible (1.75 g/l) by adding further reactant at regular intervals. Samples for analysis were removed periodically.

*p*Ap was determined by a method similar to that described by Harwood *et al*[12]. The nitrobenzene and aniline was extracted by solvents from the neutralised (pH 6) sample after it had been heated to 70°C for 30 min to ensure that all the phenylhydroxylamine had been converted to *p*Ap. The amount of *p*Ap in the aqueous phase was measured by means of a Pye–Unicam SP.800 *uv* spectrophotometer. The nitrobenzene and aniline were determined by GLC using a 2 m long Century 103 column at 198°C.

THEORETICAL

The complexity of model required to account for the behaviour of a PFTE depends on two circumstances. Firstly, whether current and electrolyte flow are in parallel or at right angles to each other. Secondly, whether significant concentration changes of reactant occur either per pass through the cell or in the direction of current flow. If these concentration changes cannot be ignored then for the flow-by configuration a two-dimensional model is required. In the present work concentration changes per pass and in the direction of current flow are negligible and hence a simple one-dimensional model proposed by Newman and Tobias[13] has been used.

This model regards the particulate and electrolyte phase as coincident continuum and assumes the applicability of Ohm's law to both. Additionally, the electrode reaction is considered to be activation controlled and capable of being described by a "high field" Tafel approximation. Under these conditions it is possible to obtain an analytical relationship[13] between a dimensionless current density j and a dimensionless distance y in the direction of current flow as:

$$j = \frac{2\theta}{\delta}\tan(\theta y - \psi) + \frac{\varepsilon}{\delta} \tag{1}$$

where θ and ψ are integration constants found by trial and error and given by

$$\tan\theta = \frac{2\delta\theta}{4\theta^2 - \varepsilon(\delta - \varepsilon)} \tag{2}$$

$$\tan\psi = \varepsilon/2\theta \tag{3}$$

δ and ε are useful dimensionless parameters characterising electrode performance and are expressed as:

$$\delta = Li\beta[1/K_s + 1/K_m] \tag{4}$$

$$\varepsilon = Li\beta/K_s \tag{5}$$

where L is the width of the electrode in the direction of current flow, i the current density based on projected cross-sectional area and $\beta = nF/RT$, $1/K_s$ and $1/K_m$ being the effective resistivity of the electrolyte and particulate phase respectively. Both δ and ε can be regarded as a ratio of reaction rate to ohmic resistivity.

For a fixed bed electrode, $1/K_m \ll 1/K_s$, *ie* $\delta = \varepsilon$. Differentiating (1) one obtains an expression for the current distribution through the electrode:

$$\frac{dj}{dy} = \frac{2\theta^2}{\delta}s^2(\theta y - \psi). \tag{6}$$

where s = sec

Since the relation of electrode potential distribution to product yield forms one of the basic objectives of the present work, it is important to be able to calculate electrode potentials in the PFTE as a function of position y. The electrode potential ϕ at any point in the electrode can be expressed as:

$$\phi = \phi_m - \phi_s \tag{7}$$

where ϕ_m and ϕ_s are the potential in the particulate and electrolyte phase respectively.

Putting $\phi' = \beta\phi$ we can write[4]:

$$i_s/i = 1 - j = -\frac{K_s}{\beta iL}(d\phi'_s/dy). \tag{8}$$

Substituting for j in (8) and integrating the resulting expression between $y = 0$ and y ($\phi'_s = 0$ at $y = 0$) and rearranging, one gets:

$$(\phi'_s)_y = \frac{2\varepsilon}{\delta}\log_e\frac{\cos(-\psi)}{\cos(\theta y - \psi)} - \frac{\varepsilon(\delta - \varepsilon)}{\delta}y. \tag{9}$$

The high field Tafel approximation can be written as:

$$dj/dy = \frac{Lai_o}{i}\exp[-(\phi'_m - \phi'_s)] \tag{10}$$

where a is the effective specific area of the particulate phase and i_o for a reversible reaction is termed the

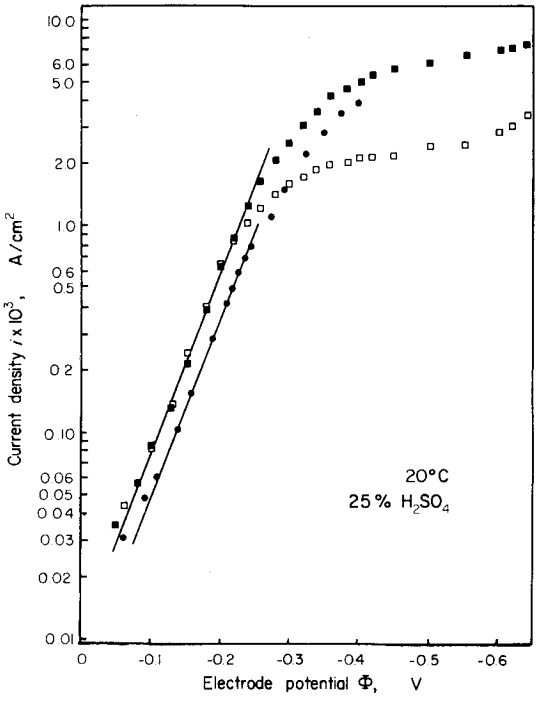

Fig. 3. Tafel plots for a planar monel cathode. ● 1.0 kg m^{-3} nitrobenzene with fluidised glass beads. □ 2.0 kg m^{-3} nitrobenzene without fluidised glass beads. ■ 2.0 kg m^{-3} nitrobenzene with fluidised glass beads.

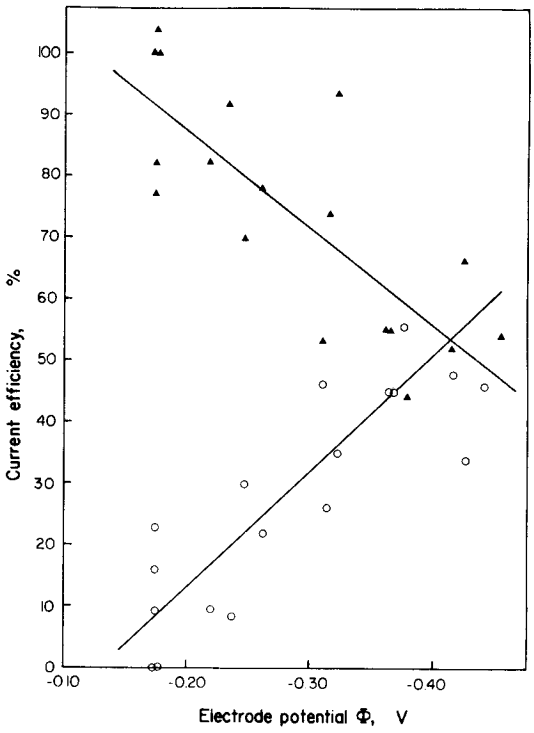

Fig. 4. Current efficiency for *p*Ap and aniline production. ▲ *p*Ap, ○ aniline, ——— least squares fit.

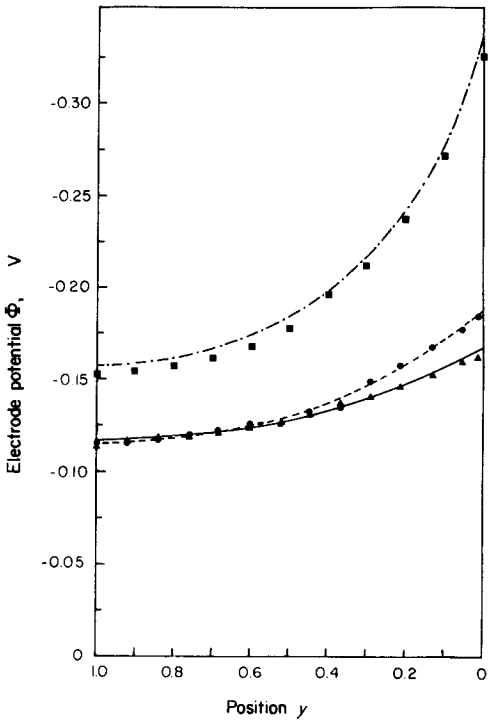

Fig. 5. Experimental and calculated potential profiles. ▲ 9.8 × 10^{-3} A/cm^2; ——— $\delta = 2.50, v = 0.40$. ● 13.6 × 10^{-3} A/cm^2; – – – $\delta = 3.45, v = 0.46$. ■ 65.5 × 10^{-3} A/cm^2; – · – $\delta = 16.6, v = 0.41$.

exchange current density. In the present case i_o merely signifies a current density determined experimentally by extrapolating the linear portion of the Tafel plot. Equating (6) and (10) and solving for ϕ', one obtains:

$$\phi'_m - \phi'_s = \log_e\left[\frac{v^2\{1+\cos(2\theta y - 2\psi)\}}{4\theta^2}\right] \quad (11)$$

where v is a dimensionless group, analogous to δ and ε and is given by:

$$v^2 = \frac{ai_oL}{i}\delta. \quad (12)$$

RESULTS AND DISCUSSION

Figure 3 shows Tafel plots for a planar monel cathode. Over a considerable potential range the plot is linear and independent of mass transfer effects since the current density in that range is unaffected by the presence of fluidised glass beads. From the slope, taking α as 0.5, n appears to be unity. Values for i_o are 6 × 10^{-6} and 10^{-5} A/cm^2 for the 1.0 and 2.0 kg m^{-3} concentrations of nitrobenzene respectively. Beyond −0.25 V the reaction becomes affected by mass transfer, reaching eventually a limiting current. Hydrogen evolution is insignificant up to a potential of −0.5 V.

Figure 4 shows corresponding current efficiencies for *p*Ap and aniline, again at the planar monel cathode in the presence of fluidised glass beads. As indicated previously, within experimental error hydrogen evolution appears to be negligible and current efficiencies add up to 100%.

Potential profiles in fixed beds

Figure 5 gives a comparison between experimentally determined values of ϕ for positions 20 cm above the electrolyte distributor and electrode potentials calculated from the model. It was found that for positions less than 10 cm above the distributor experimental values of ϕ were consistently lower although the general shape of the curves was that shown in Fig. 5. In all cases ϕ_m was essentially constant with y, justifying the assumption that $\delta = \varepsilon$. Values of δ and v used for obtaining the calculated curves, were derived from the linear portion in Fig. 3.

It will be noted that the potential distributions are predicted by the model with reasonable accuracy. As expected, activity increases rapidly as the diaphragm is approached. Also, as δ decreases electrode potentials become more uniform. The concept of a, the specific effective particulate area, arising out of (10) is discussed in the next section.

Current distribution in fixed beds

An alternative way of characterising the behaviour of a fixed bed electrode is in terms of the current distribution (see Fig. 6) in the direction y. To obtain experimental current distributions, dj/dy, a local current density, i_y, is calculated from polarisation curves for the planar electrode. For potentials high enough to indicate the presence of mass transfer effects, i_y is modified[4] by allowing for the better mass transfer occuring in the fixed bed compared with that at the planar electrode, even in the presence of the fluidised glass beads.

Returning to the local reaction activity, one can write:

$$dj/dy = \frac{Li_y a}{i} \tag{13}$$

where a is again the specific effective electrode area already seen in (10). It is obtained by multiplying the specific particulate geometric area a_o by an effectiveness factor e.

Integrating (13) between $y = 0$ and 1, one gets:

$$j = \int_0^1 \frac{a_o e L i_y \, dy}{i}. \tag{14}$$

Values of e are determined from the ratio of the measured current density at $y = 1$ to that obtained from (14) on the basis of $e = 1$. This procedure is justified since a value of $e = 0.6$ was obtained for all results[4]. This agrees well with the value of 0.5 given by Goodridge and Ismail[14] for an inorganic reaction and 0.6 obtained by Ayre[3] for an organic reduction. Experimental points in Fig. 6 again refer to a position 20 cm above the electrolyte distributor.

Looking at Fig. 6 values of dj/dy calculated from (6) agree well with experimental points. It is evident that in practice there is a clear limitation to the width of the PFTE in the direction of current flow, since activities near the feeder are relatively low.

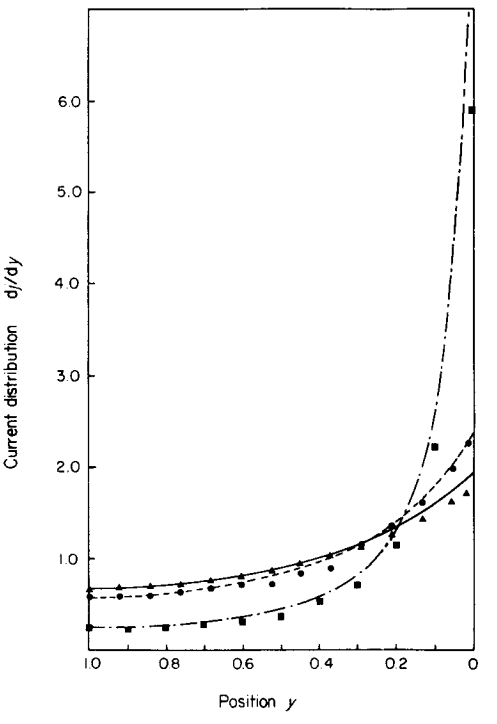

Fig. 6. Experimental and calculated current distributions. ▲ 9.8 × 10^{-3} A/cm^2; ——— $\delta = 2.50$. ● 13.6 × 10^{-3} A/cm^2; – – – $\delta = 3.45$. ■ 65.5 × 10^{-3} A/cm^2; – · – $\delta = 16.6$.

Product distribution in fixed beds

Figure 7 gives experimental current efficiencies for the production of *p*Ap and aniline. Since these add up to 100 per cent and as no major by-products were found, one can equate these current efficiencies with chemical yield. Unfortunately, it was not possible to confirm this by a sufficiently accurate mass balance since it was found that in the absence of any current, nitrobenzene was lost by adsorption onto pipe and vessel walls.

Current efficiencies (%) for *p*Ap produced at a planar monel electrode, based on the least square values of Fig. 4, can be expressed as:

$$\%\ \text{C.E.} = 119 + 158\,\phi. \tag{15}$$

Using this result for the calculation of the % C.E. for the PFTE, one gets:

$$\%\ \text{C.E.} = \frac{\int_0^1 (119 + 158\,\phi) i_y \, dy}{\int_0^1 i_y \, dy}. \tag{16}$$

Substitution of values of ϕ from Fig. 5 into (16) produces current efficiencies (see Fig. 8) that fall within the experimental uncertainty of the data obtained by direct chemical analysis (solid line in Fig. 8).

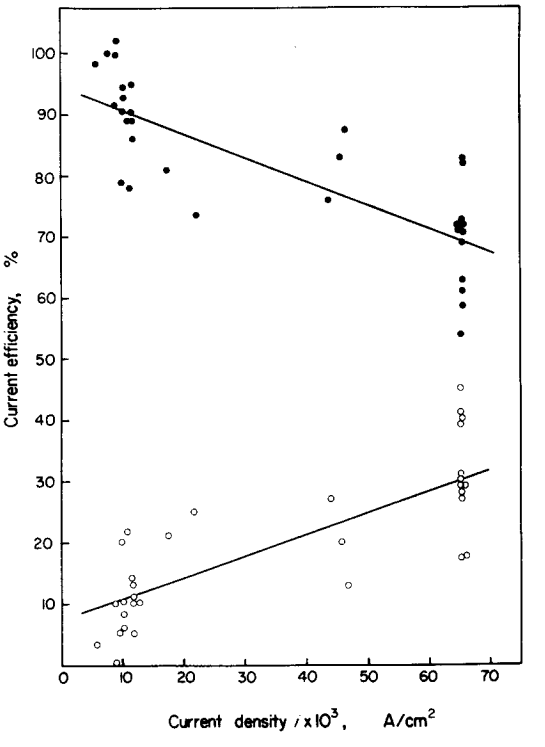

Fig. 7. Experimental current efficiencies. ● *p*Ap, ○ aniline, ——— least squares fit.

CONCLUSIONS

It is shown that the product distribution in a PFTE can be predicted from results obtained at a planar electrode. It is also found that the behaviour of a PFTE for a reaction in an essentially activation controlled regime is satisfactorily explained by a simple one-dimensional analytical model, provided concentration

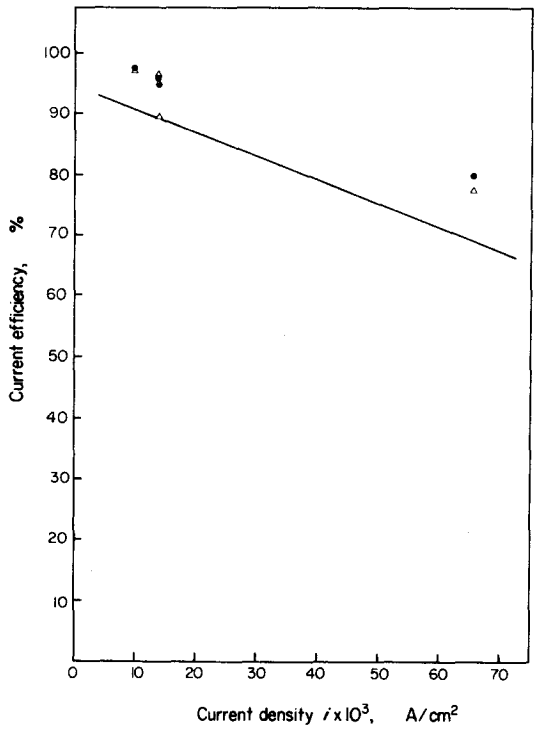

Fig. 8. Comparison between experimental and calculated current efficiencies for *p*Ap. ● calculated from experimental potential profiles. △ calculated from computed potential profiles. ——— experimental least squares fit from Fig. 7.

changes per cell pass and in the direction of current flow can be considered negligible.

Acknowledgements – One of us (M.A.H.) would like to thank the Association of Commonwealth Universities for the award of a Commonwealth Scholarship. We should also like to thank our technical staff for producing equipment of exceptionally high quality.

REFERENCES

1. R. M. Kovach, Ph.D. Thesis, Ohio State University, U.S.A. (1968).
2. P. J. Ayre, Ph.D. Thesis, University of Newcastle upon Tyne, U.K. (1973).
3. S. Yoshizawa, Z. Takehara, Z. Ogumi and T. Tsuji, *Bull. chem. Soc. Japan* **49,** 2889 (1976).
4. M. A. Hamilton, Ph.D. Thesis, University of Newcastle upon Tyne, U.K. (1979).
5. C. L. Wilson and H. V. Udupa, *J. electrochem. Soc.* **99,** 289 (1952).
6. B. B. Dey, T. R. Govindachari and S. C. Rajagopalan, *J. sci. ind. Res. (India)* **4,** 559 (1946).
7. A. Korczynski and R. Dylewski, *Przem. Chem.* **48,** 156 (1969).
8. O. Klug, *Magyar Kem. Lapja.* **15,** 535 (1960).
9. M. Fleischmann, I. N. Petrov and W. F. K. Wynne-Jones, *Proc. 1st Australian Conf. Electrochem.* p. 500, Pergamon Press, London (1965).
10. J. M. Guegeun and A. Tallec, *C.r. hebd. Séanc. Acad. Sci. Paris* **268C,** 2042 (1969).
11. Permelec S.p.A., Via Dei Canzi, 11-20134 Milano, Italy.
12. W. H. Harwood, R. M. Hurd and W. H. Jordan Jr., *I. & E.C. Process Design and Dev.* **2,** 72 (1963).
13. J. S. Newman and C. W. Tobias, *J. electrochem. Soc.* **109,** 1183 (1962).
14. F. Goodridge and B. M. Ismail, *Symposium on Electrochemical Engineering 1971*, Instn. Chem. Engrs. Symposium Series **37**(1), 29 (1973).